Anzai, H., Murkakami, T., Imai, S., Satoh, A., Nagaoka, K., & Thompson, C. J. (1987) *J. Bacteriol. 169*, 3482.
Barry, R. J., Bowman, E., McQueney, M., & Dunaway-Mariano, D. (1988) *Biochem. Biophys. Res. Commun. 153*, 177.
Bencze, W. L., & Schmid, K. (1957) *Anal. Chem. 29*, 1193.
Bowman, E., McQueney, M., Barry, R. J., & Dunaway-Mariano, D. (1988) *J. Am. Chem. Soc. 110*, 5575.
Cleland, W. W. (1979) *Methods Enzymol. 63*, 84.
Dixon, M., & Webb, E. C. (1979) *Enzymes*, 3rd ed., p 92, Academic Press, New York.
Hidaka, T., & Seto, H. (1989) *J. Am. Chem. Soc. 111*, 8012.
Hidaka, T., Mori, M., Imai, S., Hara, O., Nagaoka, K., & Seto, H. (1989) *J. Antibiot. 42*, 491.
Hilderbrand, R. C., Ed. (1983) *The Role of Phosphonates in Living Systems*, CRC Press, Boca Raton, FL.
Hori, T., Horiguchi, M., & Haysohi, A. (1984) in *Biochemistry of Natural C–P Compounds*, Maruzen, Tokyo.
Horiguchi, M., & Kandatsu, M. (1959) *Nature 184*, 901.
Klapper, M. H. (1977) *Biochem. Biophys. Res. Commun. 78*, 1018.
Mastalerz, P. (1984) in *Natural Products Chemistry* (Zalewski, R. I., & Skolik, J. J., Eds.) Elsevier, Amsterdam.
Pecoraro, U. L., Hermes, J. D., & Cleland, W. W. (1984) *Biochemistry 23*, 5262.
Schendel, P. F., & Wells, R. D. (1973) *J. Biol. Chem. 248*, 8319.
Seidel, H. M., Freeman, S., Seto, H., & Knowles, J. R. (1988) *Nature 335*, 457.
Seto, H. (1986) in *Mycotoxins and Phycotoxins* (Steyn, P. S., & Vleggaar, R., Eds.) p 77, Elsevier, Amsterdam.
Trebst, A., & Geike, F. (1967) *Z. Naturforsch. 22b*, 989.

Differential Scanning Calorimetry Study of Mixed-Chain Phosphatidylcholines with a Common Molecular Weight Identical with Diheptadecanoylphosphatidylcholine†

Hai-nan Lin, Zhao-qing Wang, and Ching-hsien Huang*
Department of Biochemistry, Health Sciences Center, University of Virginia, Charlottesville, Virginia 22908
Received December 20, 1989; Revised Manuscript Received April 20, 1990

ABSTRACT: To examine the thermotropic phase behavior of various mixed-chain phosphatidylcholines in excess water and to compare it with the known behavior of identical-chain phosphatidylcholines, we have carried out high-resolution differential scanning calorimetric (DSC) studies on aqueous dispersions of 10 different mixed-chain phosphatidylcholines. These lipids, C(16):C(18)PC, C(18):C(16)PC, C(15):C(19)PC, C(19):C(15)PC, C(14):C(20)PC, C(20):C(14)PC, C(13):C(21)PC, C(21):C(13)PC, C(12):C(22)PC, and C(22):C(12)PC, have a common molecular weight which is the same as that of C(17):C(17)PC, an identical-chain phosphatidylcholine with a molecular weight of 762.2. When the values of any of the thermodynamic parameters (T_m, ΔH, and ΔS) of the mixed-chain phosphatidylcholines and C(17):C(17)PC are plotted against the normalized chain-length difference ($\Delta C/CL$), a linear function with negative slope is obtained provided that the value of $\Delta C/CL$ is within the range of 0.09–0.4. The linear relationship suggests that these mixed-chain phospholipids are packed in the gel-state bilayer similar to the bilayer structure of C(17):C(17)PC at $T < T_m$; however, the negative slope suggests that the conformational statistics of the hydrocarbon chain and the lateral lipid–lipid interactions of these phosphatidylcholines in the gel-state bilayer are perturbed proportionally by a progressive increase in the chain-length inequivalence between the two acyl chains within each lipid molecule. When the value of $\Delta C/CL$ for mixed-chain phosphatidylcholines reaches the range of 0.44–0.55, the thermotropic phase behavior deviates markedly from that of less asymmetric phosphatidylcholines, suggesting that these highly asymmetric lipids are packed into mixed interdigitated bilayers at $T < T_m$. The heating and cooling pathways of aqueous dispersions prepared from the 10 mixed-chain phospholipids are also discussed.

In recent years, high-resolution differential scanning calorimetry (DSC)[1] has been widely used to characterize the thermotropic phase behavior of aqueous dispersions of mixed-chain phospholipids [for a recent review, see Huang and Mason (1986)]. In most of these DSC studies, however, the calorimetric experiments were carried out primarily in an ascending temperature mode. Although calorimetric cooling scans of aqueous dispersions of mixed-chain phospholipids were known for quite a few lipid species (Boggs & Mason, 1986; Mattai et al., 1987), they were limited to runs performed at relatively high scanning rates. Now, high-resolution DSC instruments with cooling scan capability are commercially available. This new accessory enables us to scan the aqueous lipid sample in both the ascending and descending temperature modes at low scanning rates; consequently, the phase transition

† This research was supported in part by U.S. Public Health Service Grant GM-17452 from the National Institute of General Medical Sciences, NIH, Department of Health and Human Services. This paper is dedicated to Professor T. E. Thompson on the occasion of his 65th birthday.

[1] Abbreviations: C(*X*):C(*Y*)PC, saturated L-α-phosphatidylcholine having *X* carbons in the *sn*-1 acyl chain and *Y* carbons in the *sn*-2 acyl chain; DSC, differential scanning calorimetry.

0006-2960/90/0429-7063$02.50/0

behavior of mixed-chain phospholipids in excess water can be examined sequentially by first heating and then cooling of the same sample in the high-resolution DSC instrument.

In recent DSC studies from this laboratory, we have reported the thermal behavior of various mixed-chain phosphatidylcholines in which one acyl chain in fully extended conformation is nearly twice as long as the other, and the phase diagrams for binary lipid mixtures containing these highly asymmetric phosphatidylcholines (Xu & Huang, 1987; Xu et al., 1987; Lin & Huang, 1988; Ali et al., 1988). In this paper, we have extended our previous DSC studies to include mixed-chain lipid species that are less asymmetrical. Specifically, a series of 11 phosphatidylcholines with a common molecular weight identical with that of C(17):C(17)PC has been chosen. These lipids C(17):C(17)PC, C(18):C(16)PC, C(16):C(18)-PC, C(19):C(15)PC, C(15):C(19)PC, C(20):C(14)PC, C-(14):C(20)PC, C(21):C(13)PC, C(13):C(21)PC, C(22):C-(12)PC, and C(12):C(22)PC, have various chain-length differences between their two saturated acyl chains, and each exhibits a characteristic main phase transition temperature (T_m) and transition enthalpy (ΔH). When the T_m or ΔH values are plotted against the normalized chain-length difference ($\Delta C/CL$) for this series of mixed-chain phosphatidylcholines, a linear function is obtained provided that the values of $\Delta C/CL$ are in the range of 0.09–0.4. Here, ΔC is the effective chain-length difference, in C–C bonds, between the *sn*-1 and *sn*-2 acyl chains, and CL is the effective length of the longer chain of the two acyl chains, in C–C bonds, for phosphatidylcholine molecules in the gel-state bilayer. In calculating the values of ΔC and CL, an inherent shortening of 1.5 C–C bond lengths must be taken into account for the *sn*-2 acyl chain. This shortening is caused by a sharp bend on the *sn*-2 acyl chain at the bond between C(2) and C(3) atoms for phosphatidylcholines in the gel-state bilayer (Zaccai et al., 1979). The definition of $\Delta C/CL$ and its calculation have been reviewed recently (Huang & Mason, 1986; Slater & Huang, 1988). The linear function in the T_m (or ΔH) vs $\Delta C/CL$ plot suggests that mixed-chain phosphatidylcholines with $\Delta C/CL$ values in the range of 0.09–0.4 are packed similarly to C(17):C(17)PC in the gel-state bilayer, i.e., the longer chain of the phospholipid molecule on one side of the bilayer packs end-to-end with the shorter chain of another phospholipid molecule in the opposing bilayer leaflet at $T < T_m$. When the value of $\Delta C/CL$ for mixed-chain phosphatidylcholines reaches the range of 0.44–0.55, the T_m or ΔH values of these highly asymmetric lipids deviate significantly from the linear function observed in the T_m or ΔH vs $\Delta C/CL$ plot for less asymmetric phospholipids, suggesting that these highly asymmetric phospholipids pack in a mixed-interdigitated mode in excess water at $T < T_m$. In addition to the polymorphic phase behavior, the melting as well as the cooling pathways of these mixed-chain phosphatidylcholines, in excess water, are elucidated in the present work.

Materials and Methods

Lysophosphatidylcholines were either obtained from Avanti Polar Lipids, Inc. (Birmingham, AL), or produced enzymatically by hydrolyzing the diacylphosphatidylcholines according to the method of Mason et al. (1981). Fatty acids were provided by Sigma Inc. (St. Louis, MO). Fatty acid anhydrides were purchased from Nu Chek Prep, Inc. (Elysian, MN). Other reagents and organic solvents were of reagent grade and spectroscopic grade, respectively.

Preparations of Mixed-Chain Phosphatidylcholines. Isomerically pure mixed-chain phosphatidylcholines with different saturated chains at *sn*-1 and *sn*-2 carbons of the glycerol backbone were prepared semisynthetically at room temperature by acylation of an appropriate lysophosphatidylcholine with an anhydride of the desired fatty acid in the presence of catalyst, 4-pyrrolidinopyridine, according to the procedure developed in this laboratory (Mason et al., 1981; Xu & Huang, 1987).

We have also adopted the procedure of Mena and Djerassi (1985) as an alternative method to semisynthesize mixed-chain phosphatidylcholines at room temperature. In this method, the cadmium chloride adduct of lysophosphatidylcholine was first prepared by dissolving lysophosphatidylcholine in absolute ethanol followed by the addition of cadmium chloride in 90% EtOH. After filtration, the dry white powder of the cadmium complex of lysophosphatidylcholine was subjected to acylation in dry chloroform with fatty acid anhydride in the presence of the catalyst 4-pyrrolidinopyridine. In fact, fatty acid anhydride was prepared in situ from fatty acid and dicyclohexylcarbodiimide in the same reaction mixture. The reaction was complete after stirring gently at room temperature for about 20 h. The resulting mixed-chain phosphatidylcholine was purified by column chromatography on silica gel. The column was eluted stepwise with chloroform, chloroform/MeOH (10:1), chloroform/MeOH/H_2O (150:30:2), and chloroform/MeOH/H_2O (160:40:5). The purified mixed-chain lipid was eluted off the column with chloroform/MeOH/H_2O (160:40:5). Finally, the purified phosphatidylcholine was filtered, lyophilized, and stored at −20 °C. The synthesized lipid proved to be at least 99% pure by thin-layer chromatography; the lipid concentrations were determined from the lipid phosphorus by the method of Gomori (1942).

Sample Preparation. Aqueous dispersions of phospholipids used for DSC experiments were prepared from lyophilized phospholipids dispersed in 50 mM NaCl solution (0 °C) containing 5 mM phosphate buffer and 1 mM EDTA at pH 7.4 to give a final lipid concentration in the range of 3.0–7.0 mM. The sample was heated 10–15 °C above T_m, and then cooled down to 0 °C. The heating/cooling cycle was repeated 2 or more times with constant vortexing, and the sample was then stored at 0 °C for a minimum of 3 days before use.

DSC Measurements. All DSC measurements were made with a high-resolution MC-2 differential scanning calorimeter with cooling scan capability (Microcal Inc., Northampton, MA); this instrument was interfaced to an IBM-PC computer (IBM Co., Boca Raton, FL) via the DA-2 digital system supplied by Microcal Inc. Prior to the initial DSC run, an incubation time of 90 min was allowed for the degassed sample in the sample cell. Each sample was scanned at least 4 times, two heating (scan rates 10–15 °C/h) and two cooling (scan rates 5–15 °C/h) runs. The transition temperatures and calorimetric enthalpies were evaluated by the software package provided by Microcal Inc.

Results

Thermotropic Phase Behavior of C(17):C(17)PC and C-(18):C(16)PC Dispersions. Although each lipid dispersion prepared from the various phosphatidylcholines under study displays different but characteristic phase transition behavior, some fully hydrated phospholipids with similar structures do show calorimetrically a common transition pattern. In this study, dispersions of C(17):C(17)PC and C(18):C(16)PC are observed to exhibit a common transition pattern upon heating or subsequent cooling. For instance, after prolonged preincubation of these two lipid dispersions at 0 °C (≤8 weeks), they all show three endothermic transitions in the first DSC heating scans from 5 to 60 °C. The lowest temperature transitions are all absent when these dispersions are scanned

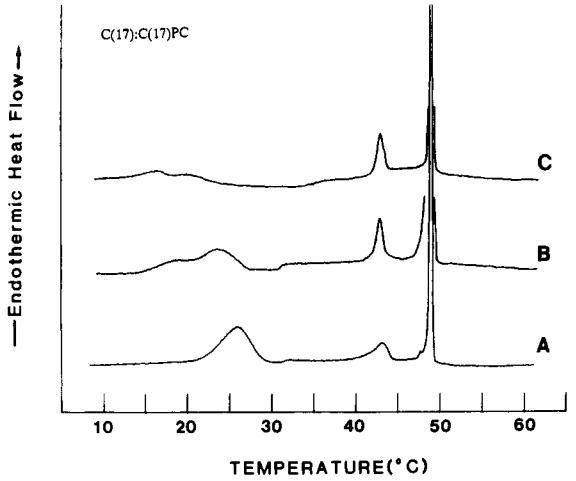

FIGURE 1: Initial DSC heating thermograms for C(17):C(17)PC dispersions. Prior to the DSC scan, the preincubation time at 0 °C for the three samples is (A) 2 months, (B) 25 days, and (C) 5 days.

subsequently to cooling from 60 °C or to immediate reheating from 5 °C.

Shown in Figure 1A is the first DSC heating thermogram for a C(17):C(17)PC dispersion that has been preincubated at 0 °C for 2 months. Three discernible endothermic transitions peaked at 25.9, 43.1, and 49.0 °C with transition enthalpy (ΔH) values of 3.8, 1.0, and 9.7 kcal/mol, respectively, are observed. The low-temperature transition at 25.9 °C is abolished upon cooling; consequently, by this criterion, the irreversible low-temperature transition can be assigned as the $L_c \rightarrow L_{\beta'}$ subtransition (Chen et al., 1980), where L_c is the crystalline phase and $L_{\beta'}$ is the tilted gel phase. If a C(17):C(17)PC dispersion is subject to preincubation at 0 °C for 5 days, the first heating thermogram shows four discernible endothermic transitions; these endotherms are peaked at 16.4, 19.9, 42.4, and 49.0 °C as illustrated in Figure 1C. The two low-temperature transitions at 16.4 and 19.9 °C are partially overlapped with a total transition enthalpy of about 2.3 kcal/mol; furthermore, they are irreversible on cooling and immediate reheating. An additional DSC experiment carried out with a C(17):C(17)PC dispersion that has been stored at 0 °C for 25 days indicates that the two overlapped low-temperature transitions are shifted upward, peaked at 17.5 and 23.1 °C (Figure 1B). These DSC heating thermograms clearly indicate that the transition temperatures of the two overlapped peaks observed for C(17):C(17)PC dispersions increase with increasing preincubation time at 0 °C, and the two low-temperature transitions merge into a single broad peak after incubating at 0 °C for extended periods (≥8 weeks). A similar thermotropic behavior has also been observed for the C(16):C(16)PC subtransition composed of two overlapped components (Wu et al., 1985). These two overlapped low-temperature peaks exhibited by C(17):C(17)PC dispersions can thus be assigned as subtransitions. In fact, this assignment was first given by Finefold and Singer (1984).

The small transition at about 43 °C for C(17):C(17)PC dispersions is detectable in both the first heating and first cooling DSC curves. This is the pretransition, corresponding to the $L_{\beta'} \rightarrow P_{\beta'}$ transition, where $L_{\beta'}$ is the tilted gel phase and $P_{\beta'}$ is the periodic ripple phase.

The high-temperature transition for C(17):C(17)PC dispersions at 49.0 °C with $\Delta H = 9.7 \pm 0.2$ kcal/mol is the main phase transition, corresponding to the $P_{\beta'} \rightarrow L_\alpha$ phase transition, where L_α is the liquid-crystalline or fluid phase. The transition characteristics of this main phase transition are independent of the thermal history of the sample. This main

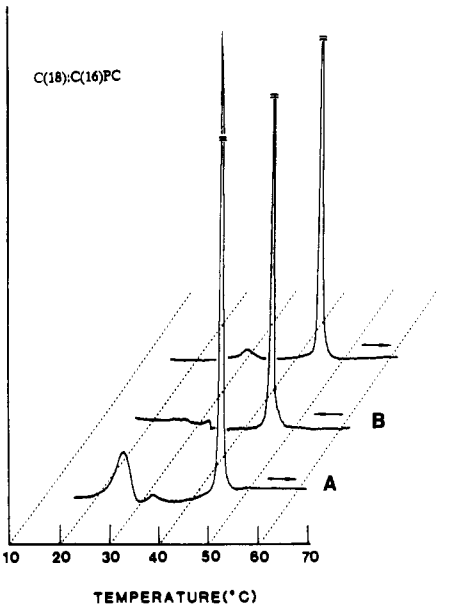

FIGURE 2: Successive DSC thermograms for a C(18):C(16)PC dispersion which has been preincubated at 0 °C for 7 days. (A) The initial heating thermogram; (B) the first cooling thermogram; (C) the second heating thermogram. Arrows show the direction of temperature change.

transition behavior has been reported previously (Finegold & Singer, 1984; Lewis et al., 1987).

The first heating, cooling, and the second heating DSC thermograms for C(18):C(16)PC dispersions in the temperature range of 15–60 °C are illustrated in Figure 2. Similar to C(17):C(17)PC dispersions, three discernible endotherms can be seen in the first DSC heating thermogram (Figure 2A). These transitions are peaked at 24.5 °C (ΔH = 3.3 kcal/mol), 30.4 °C (ΔH = 0.3 kcal/mol), and 44.4 °C (ΔH = 9.0 kcal/mol). The broad low-temperature transition at 24.5 °C is abolished in the cooling and reheating curves (Figure 2B,C), a behavior again similar to that of C(17):C(17)PC dispersions. The three endothermic transitions observed in the first heating curve, being of the same transition pattern as that exhibited by prolonged incubated (≥8 weeks at 0 °C) C(17):C(17)PC dispersions, can be attributed to the subtransition ($L_c \rightarrow L_{\beta'}$), the pretransition ($L_{\beta'} \rightarrow P_{\beta'}$), and the main phase transition ($P_{\beta'} \rightarrow L_\alpha$), respectively.

Thermotropic Phase Behavior of C(16):C(18)PC, C(15):C(19)PC, C(19):C(15)PC, and C(14):C(20)PC Dispersions. Aqueous dispersions of C(16):C(18)PC, C(15):C(19)PC, C(19):C(15)PC, and C(14):C(20)PC that have been stored at 0 °C for more than 3 days all exhibit calorimetrically a common transition pattern on either heating or subsequent cooling. The first DSC heating scans of these dispersions are characterized by two prominent well-resolved endothermic transitions: a broad endotherm occurring at a lower temperature and a sharp one at a higher temperature. Upon cooling from above the transition temperature of the high-temperature endotherm or immediate reheating after cooling, the broad low-temperature transition disappears in all the thermograms obtained from dispersions prepared from these four mixed-chain phosphatidylcholines.

The first DSC heating thermogram for an aqueous dispersion of C(16):C(18)PC that has been annealed at 0 °C for 40 days is shown in Figure 3A. The low-temperature broad transition is peaked at 36.8 °C (ΔH = 4.8 kcal/mol), and the high-temperature sharp transition is peaked at 48.8 °C (9.8 kcal/mol). The appearance of only two endotherms for the annealed sample is unexpected, since an observation of three

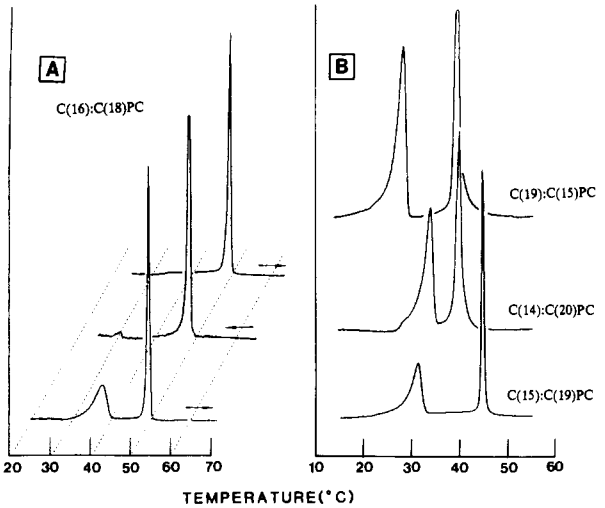

FIGURE 3: (A) Successive DSC thermograms for a C(16):C(18)PC dispersion that has been preincubated at 0 °C for 40 days. The bottom trace is the initial heating scan; the middle trace is the first cooling scan; the upper trace is the immediate second heating scan. (B) The initial heating thermograms for C(15):C(19)PC (bottom trace), C(14):C(20)PC (middle trace), and C(19):C(15)PC dispersions.

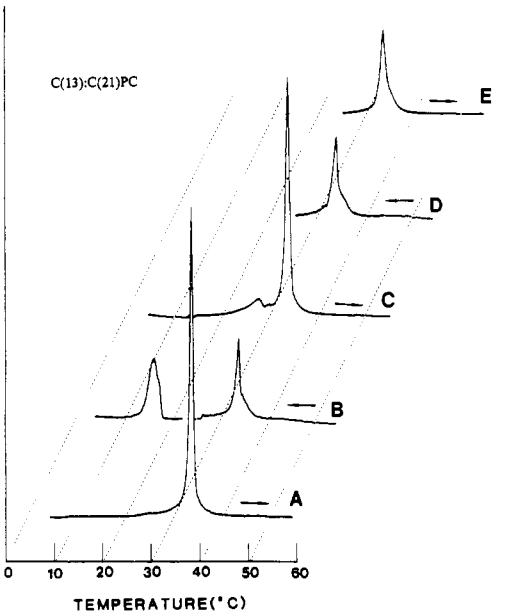

FIGURE 4: DSC thermograms for C(13):C(21)PC dispersions. Traces A–C show the successive heating, cooling, and reheating curves of the same sample in the temperature range of 10–55 °C. Traces D and E illustrate the cooling and reheating curves recorded in the temperature range of 25–55 °C.

endothermic transitions at 37.5, 40.6, and 49.3 °C has been reported for annealed samples of fully hydrated C(16):C(18)PC (Mattai et al., 1987). However, repeated DSC experiments with annealed samples of C(16):C(18)PC prepared in this laboratory fail to detect the 40.6 °C transition, and we do not know the origin of this discrepancy.

The cooling and immediate reheating thermograms for aqueous dispersions of C(16):C(18)PC in the temperature range of 25–65 °C are also illustrated in Figure 3A. In both curves, a sharp, major transitions peaked at 48.8 °C is observed. This transition corresponds to the high-temperature transition observed in the initial DSC heating thermogram. The apparent absence of the low-temperature transition at 36.8 °C on cooling indicates that this transition can be attributed to the subtransition. If the reheating scan is carried out after the sample has been incubated in the calorimetric cell for 1 h at 15 °C, a broad transition at 35.2 °C with a small enthalpy (ΔH = 2.2 kcal/mol) can be detected, indicating that the subtransition seen in the first DSC heating scan reappears partially under the experimental conditions.

For annealed samples of C(15):C(19)PC, C(14):C(20)PC, and C(19):C(15)PC dispersions, the general pattern of their first DSC heating curves is identical with that of C(16):C(18)PC dispersions, which is characterized by two well-resolved endothermic transitions as illustrated in Figure 3B. The peak temperatures of the low-temperature broad transitions for C(15):C(19)PC, C(14):C(20)PC, and C(19):C(15)PC dispersions occur at 31.3 °C (ΔH = 4.1 kcal/mol), 33.9 °C (ΔH = 7.6 kcal/mol), and 28.3 °C (ΔH = 6.8 kcal/mol), respectively. These low-temperature transitions all disappear on subsequent cooling and immediate reheating (data not shown). The high-temperature transition peaks for C(15):C(19)PC, C(14):C(20)PC, and C(19):C(15)PC dispersions are considerably sharper with peak maxima occurring at 44.8 °C (ΔH = 9.1 kcal/mol), 40.0 °C (ΔH = 7.5 kcal/mol), and 39.0 °C (ΔH = 7.1 kcal/mol), respectively. These high-temperature transitions are clearly the main phase transitions which remain in their entireties upon subsequent cooling or immediate reheating. X-ray diffraction data obtained with fully hydrated C(16):C(18)PC on heating show the appearance of three different phases, L_c, $P_{\beta'}$, and L_α (Stümpel et al., 1983; Mattai et al., 1987). Consequently, the subtransition and the main phase transition observed for C(16):C(18)PC dispersions can be ascribed to the $L_c \rightarrow P_{\beta'}$ and the $P_{\beta'} \rightarrow L_\alpha$ phase transitions, respectively, (Mattai et al., 1987). Since the phase transition behavior of C(15):C(19)PC, C(14):C(20)PC, and C(19):C(15)PC dispersions is of the same pattern as that of the C(16):C(18)PC dispersion, the low-temperature and high-temperature transitions observed for dispersions of these lipids in the first DSC heating scan can be reasonably assigned as the $L_c \rightarrow P_{\beta'}$ and the $P_{\beta'} \rightarrow L_\alpha$ phase transitions, respectively. Similarly, the single transition detected in the cooling mode may be attributed to the $L_\alpha \rightarrow P_{\beta'}$ transition.

Thermotropic Phase Behavior of C(13):C(21)PC Dispersions. Figure 4A–C shows the successive heating, cooling, and reheating thermograms for an example of C(13):C(21)PC dispersions that has been annealed at 0 °C for 7 days. A sharp endothermic transition peaked at 34.1 °C is observed on initial heating from 5 to 55 °C. Interestingly, this endothermic transition exhibits an unusually large value of ΔH of 17.7 ± 0.5 kcal/mol. In contrast, two well-resolved exotherms peaked at 33.8 °C (ΔH = 5.5 kcal/mol) and 16.4 °C (ΔH = 7.9 kcal/mol) are seen on cooling from 55 to 5 °C. Immediate reheating of the same sample shows two endotherms: a small transition at 28.1 °C (ΔH = 1.1 kcal/mol) and a sharp symmetric transition at 34.1 °C with considerably greater enthalpy (ΔH = 14.9 kcal/mol).

Figure 4D shows the DSC thermogram for a C(13):C(21)PC sample scanned in the descending temperature mode from 55 to 25 °C; it exhibits a single transition at 34.0 °C (ΔH = 5.5 kcal/mol). Reheating of the same sample gives an endotherm at 33.8 °C with a ΔH of 6.2 kcal/mol (Figure 4E), demonstrating that the high-temperature exotherm observed in the initial cooling scan, shown in Figure 4B, is reversible. Consequently, the extraordinarily large endotherm (ΔH = 17.7 kcal/mol) observed in the first DSC heating run of C(13):C(21)PC dispersions is most likely to be caused by a superposition of two phase transitions which can be decoupled into two well-resolved exotherms upon cooling. This endothermic transition observed in the initial DSC scan can be assigned tentatively as the $L_c \rightarrow L_\alpha$ phase transition. This assignment

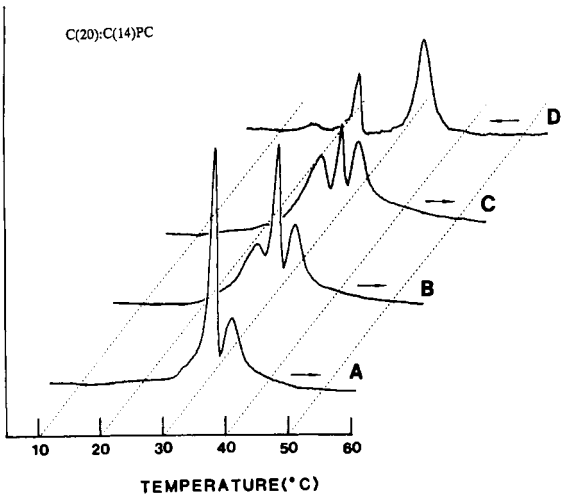

FIGURE 5: Three successive heating and cooling thermograms for C(20):C(14)PC dispersions recorded in the temperature range of 5–50 °C. The preincubation times at 0 °C prior to the three heating runs of the same sample are (A) 10 days, (B) 150 min, and (C) 50 min. The uppermost trace represents a typical cooling curve. In order to show the minor exothermic transition at 15 °C, the cooling trace is drawn to an expanded scale (×1.6).

is not unreasonable, since a direct conversion from the L_c phase to the L_α phase has been previously observed for annealed samples of C(13):C(13)PC dispersions (Lewis et al., 1987). The two exotherms appeared in the cooling scan may be assigned as the $L_\alpha \rightarrow P_{\beta'}$ transition (high-termperature) and the $P_{\beta'} \rightarrow L_c$ phase transition (low-temperature). The calorimetric detection of $P_{\beta'} \rightarrow L_c$ is unusual, since the formation of the L_c phase ordinarily requires a long annealing of the lipid sample such as C(16):C(16)PC at low temperatures. However, the $P_{\beta'}$ phase is known to be very unstable for short-chain lipids such as C(13):C(13)PC (Lewis et al., 1987). It is quite possible that the $P_{\beta'}$ phase in C(13):C(21)PC is also extremely unstable; consequently, the formation of the L_c phase proceeds much more quickly than that of longer identical-chain lipids. Further detailed studies utilizing other physical techniques are needed to confirm our assignments.

Thermotropic Phase Behavior of C(20):C(14)PC Dispersions. The phase behavior of C(20):C(14)PC dispersions exhibited in the DSC heating thermogram depends heavily on the thermal history of the lipid sample, although the cooling scan displays virtually identical results in all samples. Figure 5 shows three successive heating thermograms and a typical example of a cooling thermogram obtained within the temperature interval of 5–50 °C. Curve A is the initial heating thermogram of a sample that has been preincubated at 0 °C for 10 days; it is characterized by two partially overlapped features peaked at 30.4 °C ($\Delta H \simeq 9.5$ kcal/mol) and 33.2 °C ($\Delta H \simeq 4.0$ kcal/mol). Curve B is the second heating thermogram of the same sample, performed after cooling it in the calorimetric cell from 50 to 5 °C and incubating at 5 °C for 150 min. This curve displays three partially overlapped endothermic transitions peaked at 27.0, 30.4, and 33.2 °C. The third heating thermogram, performed after incubating the same sample at 5 °C for 50 min, also shows three partially overlapped endotherms at 27.0, 30.4, and 33.2 °C (curve C in Figure 5); however, the peak areas under the low- and mid-temperature transitions are significantly different from those shown in the second heating curve. The DSC cooling curve, shown in Figure 5D, is characterized by three exotherms at 33.2 °C (ΔH = 4.7 kcal/mol), 22.8 °C (ΔH = 1.2 kcal/mol), and 15 °C ($\Delta H \simeq 0.3$ kcal/mol).

Since the high-temperature endotherm at 33.2 °C is reversible on cooling, and since the enthalpy change associated with this transition is independent of the thermal history of the sample (Figure 5A–C), this phase transition can be assigned as the $P_{\beta'} \rightarrow L_\alpha$ phase transition. Comparing the heating thermograms obtained with increasing preincubation times, it is evident that the area under the low-temperature transition at 27 °C decreases concomitantly with an increase in the area under the mid-temperature transition at 30.4 °C. This calorimetric behavior immediately suggests that the low-temperature endotherm at 27 °C involves a phase transition of lamellar C(20):C(14)PC from a metastable state, and the metastable state is converted slowly at 5 °C to a more stable state which is responsible for the mid-temperature endothermic transition at 30.4 °C. Furthermore, both the low- and mid-temperature transitions are irreversible on cooling. We may, therefore, attribute this mid-temperature transition at 30.4 °C to the $L_c \rightarrow P_{\beta'}$ phase transition. Similarly, the low-temperature transition at 27 °C can be ascribed to the metastable $L_{gel}^{MI} \rightarrow P_{\beta'}$ phase transition, where L_{gel}^{MI} is the mixed-interdigitated gel phase (vide post). It should be noted that the peak positions of the two partially overlapped transitions at 27 and 30.4 °C, shown in Figure 5A–C, are not shifted as the preincubation time increases; hence, these transitions are different from those two subtransitions initially observed for C(17):C(17)PC as illustrated in Figure 1.

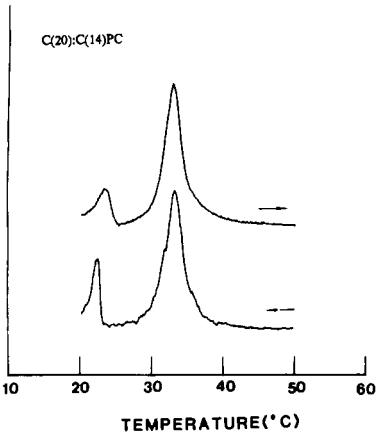

FIGURE 6: Cooling and immediate reheating DSC curves of a C(20):C(14)PC dispersion recorded in the temperature range of 20–50 °C.

The DSC cooling and reheating thermograms for C(20):C(14)PC dispersions in the temperature interval of 20–50 °C are illustrated in Figure 6. These thermograms show that C(20):C(14)PC dispersions undergo two reversible transitions at 23.0 °C (ΔH = 1.1 kcal/mol) and 33.1 °C (ΔH = 4.3 kcal/mol). The high-temperature transition is the main phase transition which can be ascribed to the $P_{\beta'} \rightarrow L_\alpha$ phase transition as discussed earlier, and the low-temperature transition may be assigned as the pretransition, or the $L_{\beta'} \rightarrow P_{\beta'}$ transition, based on the small magnitude of ΔH associated with this transition.

A comparison of the DSC thermograms obtained in the temperature range of 5–50 °C (Figure 5) with those obtained at 20–50 °C (Figure 6) indicates that the $L_{\beta'}$ phase of lamellar C(20):C(14)PC can be transformed irreversibly at low temperatures into the stable L_c phase via the metastable gel phase L_{gel}^{MI}. Overall, the thermotropic phase behavior of C(20):C(14)PC dispersions in the temperature interval of 5–50 °C can be summarized in Scheme I.

Thermotropic Phase Behavior of C(12):C(22)PC, C(21):C(13)PC, and C(22):C(12)PC Dispersions. The aqueous dispersions of C(12):C(22)PC, C(21):C(13)PC, and C(22):

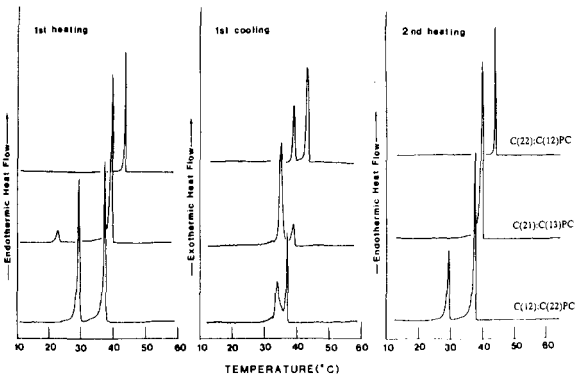

FIGURE 7: Successive DSC thermograms for aqueous dispersions of C(12):C(22)PC, C(21):C(13)PC, and C(22):C(12)PC recorded in the temperature interval of 10–60 °C. Prior to the first heating scan, the samples have been incubated at 0 °C for 3, 3, and 24 days, respectively.

Scheme I

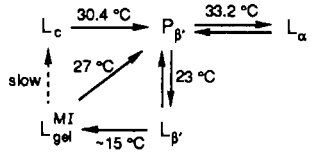

C(12)PC all exhibit a common transition pattern in their DSC cooling scans, although their heating thermograms show somewhat different patterns. Another reason we group these three lipids together is because their values of $\Delta C/CL$ are in the range of 0.44–0.55. As discussed elsewhere (Mason et al., 1981; Huang & Mason, 1986; Slater & Huang, 1988; Huang, 1990), $\Delta C/CL$ can be employed to quantitatively represent the normalized value of the chain length difference between the *sn*-1 and *sn*-2 acyl chains in a mixed-chain lipid molecule in the gel-state bilayer. On the basis of geometric considerations and also on the basis of X-ray diffraction and other DSC data of a number of mixed-chain phospholipids, it has been postulated that mixed-chain phospholipids with values of $\Delta C/CL$ in the range of 0.44–0.57 can self-assemble in excess water into mixed-interdigitated bilayers at $T < T_m$ [for a most recent review, see Huang (1990)]. The values of $\Delta C/CL$ for C(12):C(22)PC, C(21):C(13)PC, and C(22):C(12)PC are 0.44, 0.48, and 0.55, respectively; hence, it is reasonable to assume that these lipids may form, at $T < T_m$, mixed-interdigitation bilayers.

Calorimetric thermograms for a C(12):C(22)PC dispersion which, prior to the DSC run, has been annealed at 0 °C for 3 days are shown in Figure 7. The initial heating scan in the temperature range of 10–60 °C exhibits two nearly identical peaks at 29.4 °C (ΔH = 11.4 kcal/mol) and 37.5 °C (ΔH = 11.8 kcal/mol). A cooling scan from 60 to 10 °C gives two overlapped transitions at 33.8 and 36.9 °C with a total transition enthalpy of 11.8 kcal/mol. A second heating scan performed immediately after cooling exhibits two discernible transitions with a larger high-temperature endotherm (ΔH = 13.2 kcal/mol) but a smaller low-temperature endotherm (ΔH = 5.9 kcal/mol). Furthermore, in a separate experiment, the first heating scan carried out in the temperature range of 22–35 °C gives only a single endotherm at 29.4 °C which disappears in both the successive cooling and second heating runs performed within the same temperature interval of 22–35 °C. These DSC results suggest that the low-temperature endotherm at 29.4 °C is a subtransition or the $L_c^{MI} \rightarrow L_\alpha$ phase transition, where L_c^{MI} is the mixed-intedigitated crystalline phase, and that the high-temperature endotherm at 37.5 °C corresponds to the mixed-interdigitated gel $\rightarrow L_\alpha$ phase transition. A similar transition behavior has been previously reported for annealed samples of fully hydrated C(18):C(12)PC (Boggs & Mason, 1986; Mattai et al., 1987). It is interesting to note that the value of $\Delta C/CL$ for C(18):C(12)PC is 0.44, which is precisely the same value of $\Delta C/CL$ calculated for C(12):C(22)PC.

As shown in Figure 7, the cooling scan of C(12):C(22)PC dispersions displays two partially overlapped exotherms peaked at 33.8 and 36.9 °C. The ratio of the peak areas of the two exotherms observed in the first cooling scan differs from that observed in the second cooling scan; the low-temperature transition increases in magnitude at the expense of the high-temperature transition. Moreover, the total enthalpy of the two overlapped exotherms appears to remain constant (ΔH = 11.8 kcal/mol). This suggests that the formation of the mixed-interdigitated gel phase from the L_α phase may involve an intermediate gel phase, and the newly formed interdigited gel phase can subsequently promote the rapid and direct formation of more mixed-interdigitated gel phase from the L_α phase.

Also shown in Figure 7 are the DSC thermograms for a C(21):C(13)PC dispersion that has been preincubated at 0 °C for 3 days. The first heating scan performed in the temperature range of 10–60 °C shows a small transition at 22.7 °C (ΔH = 1.1 kcal/mol) and a sharp main transition peaked at 39.4 °C (ΔH = 12.0 kcal/mol). The same sample shows two partially overlapped transitions on first cooling, peaked at 34.9 °C ($\Delta H \simeq$ 8.3 kcal/mol) and 38.7 °C ($\Delta H \simeq$ 1.5 kcal/mol). Subsequent reheatings of the same sample show only the high-temperature main transition at 39.4 °C with an identical transition enthalpy of 12.0 kcal/mol. Two partially overlapped exotherms at 34.8 and 38.7 °C are detected again in the second cooling scan; the relative ratio of the peak areas for the two exotherms depends on the thermal history of the sample, a behavior also exhibited by C(12):C(22)PC dispersions as discussed earlier. Hence, the general transition pattern induced by the thermal changes for C(21):C(13)PC and C(12):C(22)PC dispersions is identical, although the associated transition temperatures and enthalpies are different.

Finally, Figure 7 also displays the DSC thermograms for an annealed sample (24 days at 0 °C) of C(22):C(12)PC dispersions. A sharp, single endothermic transition peaked at 43.4 °C (ΔH = 13.5 kcal/mol) is observed in the first heating run from 10 to 60 °C. Subsequent reheatings of the same sample give reproducible results. A similar heating behavior has also been observed for fully hydrated C(18):C(10)PC (Xu & Huang, 1987). The single transition observed in the first and second heating thermograms can be attributed to the mixed-interdigitated gel $\rightarrow L_\alpha$ phase transition (Hui et al., 1984; McIntosh et al., 1984; Boggs & Mason, 1986; Mattai et al., 1987). It should be mentioned that a common transition pattern for C(22):C(12)PC and C(18):C(10)PC dispersions is expected, since the values of $\Delta C/CL$ for C(18):C(10)PC and C(22):C(12)PC are 0.56 and 0.55, respectively, suggesting that they are packed similarly in the gel-state bilayer. On cooling, however, two exotherms at 38.6 and 42.7 °C with a total transition enthalpy of 13.0 kcal/mol are detected for C(22):C(12)PC dispersions. The area under the low-temperature exotherm increases with repeated coolings at the expense of the high-temperature exotherm. A similar cooling behavior has also been observed for C(18):C(10)PC dispersions. It appears that the high-temperature exotherm may correspond to the transition of C(22):C(12)PC from a metastable L_α state to an intermediate gel state which, in turn,

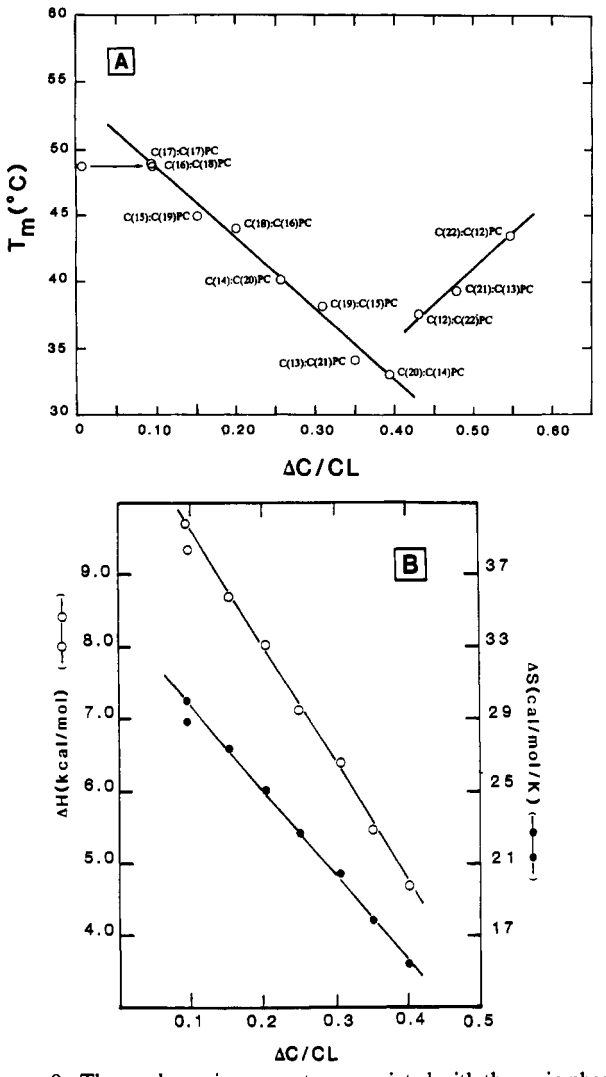

FIGURE 8: Thermodynamic parameters associated with the main phase transition for aqueous dispersions of various mixed-chain phosphatidylcholines are plotted against the normalized chain-length difference ($\Delta C/CL$) between two acyl chains in these phospholipids. (A) Transition temperature (T_m) vs $\Delta C/CL$. If a 2gl kink is introduced into the *sn*-1 acyl chain in C(16):C(18)PC, the value of $\Delta C/CL$ will be increased from 0.032 to 0.096 as indicated by the arrow. (B) ΔH and ΔS vs $\Delta C/CL$. A Δ C/CL value of 0.096 is used for C(16):C(18)PC in this figure. The values of ΔH are calculated from the exothermic peak area obtained from the DSC cooling curves as shown in Table I, and the values of ΔS are taken from Table I.

converts to the mixed-interdigitated gel phase. The newly formed interdigitated gel phase then promotes the direct conversion of lipid molecules from the stable L_α phase to the mixed-interdigitated gel state. One may further speculate that the concentration of lamellar lipids in the metastable L_α state decreases as the lamellar lipids are subjected to repeated heating/cooling cycles, leading to a reduction in the area of the high-temperature exotherm.

Discussion

In this study, the thermotropic phase behavior of a series of fully hydrated phosphatidylcholines is compared. This series of phosphatidylcholines is characterized by having a common molecular weight of 762.2. They are C(16):C(18)PC, C(17):C(17)PC, C(15):C(19)PC, C(18):C(16)PC, C(14):C(20)PC, C(19):C(15)PC, C(13):C(21)PC, C(20):C(14)PC, C(12):C(22)PC, C(21):C(13)PC, and C(22):C(12)PC.

The main phase transition temperature (T_m) of aqueous dispersions prepared from these various mixed-chain phospholipids is plotted in Figure 8 as a function of the normalized chain-length difference or inequivalence ($\Delta C/CL$). Within the range of $\Delta C/CL$ from 0.09 to 0.4, the effect of increasing progressively the chain-length inequivalence is to decrease linearly the main phase transition temperature (Figure 8A). This linear dependence of T_m upon $\Delta C/CL$ suggests that the hydrocarbon chains of lamellar phospholipids in the gel state are perturbed by the acyl chain inequivalence and that the gel-state disordering effects arising from the inequivalent chain structures are increased in proportion to the increase in the normalized chain-length difference between the *sn*-1 and *sn*-2 acyl chains. An analogous linear relationship between the chain-length inequivalence and the chain melting behavior has also been observed for lamellar identical-chain phosphatidylcholines in excess water (Mason & Huang, 1981; Huang & Levin, 1983). This similarity further suggests that mixed-chain phosphatidylcholines with $\Delta C/CL$ values in the range of 0.15–0.40 and C(17):C(17)PC ($\Delta C/C = 0.09$) are, in excess water, most likely to self-assemble into similar bilayer structures at $T < T_m$. It is thus reasonable to state that for these mixed-chain phospholipids the longer chain of the lipid on one side of the bilayer packs end-to-end with the shorter chain of another lipid molecule in the opposing bilayer leaflet at $T < T_m$.

As the values of the normalized chain-length difference between the *sn*-1 and *sn*-2 acyl chains ($\Delta C/CL$) reach the range of 0.44–0.55, Figure 8A shows that the values of T_m for C(12):C(22)PC, C(21):C(13)PC, and C(22):C(12)PC dispersions deviate significantly from the linear function of $\Delta C/CL$ vs T_m as exhibited by those less asymmetrical phospholipids. When the value of $\Delta C/CL$ for a mixed-chain phosphatidylcholine is in the neighborhood of 0.5, it means that one hydrocarbon chain of this lipid molecule in the fully extended conformation is about twice as long as the other. Phosphatidylcholines with such a high degree of asymmetry such as C(18):C(10)PC ($\Delta C/CL = 0.56$), C(18):C(12)PC ($\Delta C/CL = 0.42$), and C(8):C(18)PC ($\Delta C/CL = 0.53$) are known from X-ray diffraction data to form mixed-interdigitated gel bilayers at $T < T_m$ (Hui et al., 1984; McIntosh et al., 1984; Mattai et al., 1987; Shah et al., 1990). The observed deviation for C(12):C(22)PC, C(21):C(13)PC, and C(22):C(12)PC as shown in Figure 8A can be readily interpreted as arising from a different and more ordered molecular packing of phospholipids in the gel-state bilayer. Such a molecular packing is consistent with the mixed-interdigitated packing in which the methyl terminus of the shorter chain is packed end-to-end, at the bilayer center, with the methyl terminus of the shorter chain from another lipid molecule in the opposing bilayer leaflet, while the longer chains from the two leaflets span the entire hydrocarbon width of the bilayer (Hui et al., 1984; McIntosh et al., 1984; Mattai, et al., 1987). In fact, C(22):C(12)PC molecules have been inferred, based on thermodynamic data, to form mixed-interdigitated bilayers at $T < T_m$ (Xu & Huang, 1987) as diagramatically presented in Figure 9.

It should be noted that the T_m value for C(16):C(18)PC ($\Delta C/CL = 0.032$) also deviates from the linear function shown in Figure 8A. When the value of $\Delta C/CL$ for a mixed-chain lipid is nearly equal to zero, it means that the two acyl chains of the lipid molecule have effectively equal length. Physically, the two acyl chains with equal chain length cannot pack with an all-trans conformation in the bilayer, because the two bulky methyl terminal groups would align next to each other in the bilayer center to form an unfavorable packing situation. We propose that the shorter *sn*-1 chain, in the case of C(16):C-

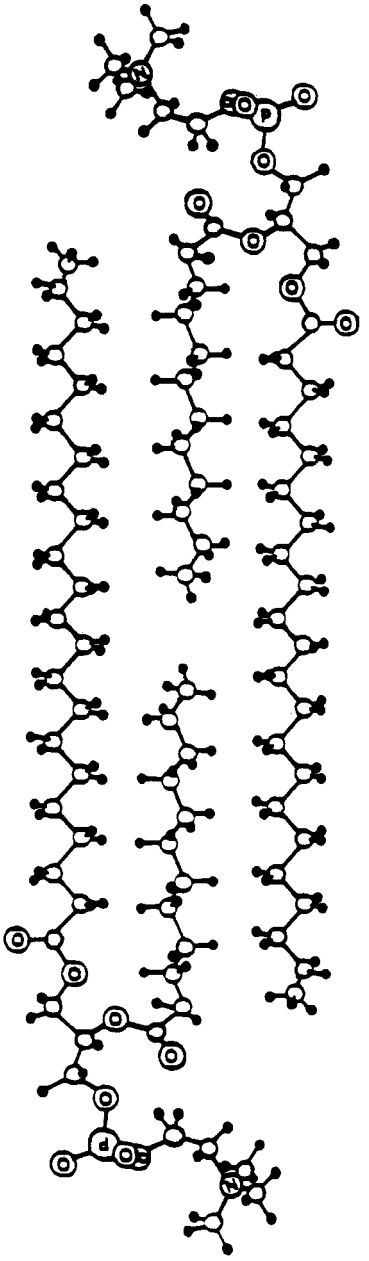

FIGURE 9: Schematic drawing to illustrate the acyl chain packing of C(22):C(12)PC in the mixed-interdigitated bilayer. The long acyl chain is shown to span the entire hydrocarbon width of the bilayer, while the two shorter chains, each from a lipid molecule in the opposing leaftlet, meet end-to-end in the bilayer mid-plane. The mixed-interdigitated packing mode for C(22):C(12)PC was inferred to take place at $T < T_m$, based on thermodynamic data of Xu and Huang (1987).

(18)PC molecules, will be further shortened by one C–C bond length by the formation of a 2gl kink so that the terminal methyl groups in the gel-state bilayer will be packed next to methylene groups rather than other methyl groups. This is a closer packing situtation; however, the $\Delta C/CL$ value is increased from 0.032 to 0.096. Interestingly, when the value of $\Delta C/CL = 0.096$ is employed for C(16):C(18)PC, the T_m value for C(16):C(18)PC falls nicely on the linear curve in Figure 8A, indicating that the proposed formation of a 2gl kink in the *sn*-1 acyl chain is not unreasonable.

The values of the transition enthalpy (ΔH) associated with the gel → liquid-crystalline phase transition for aqueous dispersions prepared from various mixed-chain phosphotidylcholines with values of $\Delta C/CL < 0.44$ can be estimated directly from the main exotherms recorded in the cooling scans.

Table I: Thermodynamic Parameters Associated with the Main Phase Transition of Mixed-Chain Phosphatidylcholine Dispersions

phosphatidylcholine	$\Delta C/CL$	T_m (°C)[a]	ΔH (kcal/mol)[a]	ΔS (cal mol^{-1} K^{-1})[a]
C(17):C(17)PC	0.09	49.0	9.7	30.1
C(16):C(18)PC	0.03 (0.1)[b]	48.8	9.3	28.9
C(15):C(19)PC	0.15	44.8	8.7	27.4
C(18):C(16)PC	0.21	44.4	8.0	25.1
C(14):C(20)PC	0.26	40.0	7.1	22.7
C(19):C(15)PC	0.31	39.0	6.4	20.5
C(13):C(21)PC	0.35	34.1	5.5	17.9
C(20):C(14)PC	0.40	33.2	4.7	15.4

[a] T_m value was taken to be the temperature of the maximal excess heat capacity recorded in the heating scan; the value of ΔH was calulated on the basis of the area of the main exotherm recorded in the cooling scans; the value of ΔS, the transition entropy, was calculated from the Clausius equality of $\Delta S = \Delta H/T_m$ assuming a first-order equilibrium transition. The experimental errors in T_m and ΔH are within 1% and 25%, respectively. [b] Calculated on the basis of the putative presence of a 2gl kink on the *sn*-1 acyl chain.

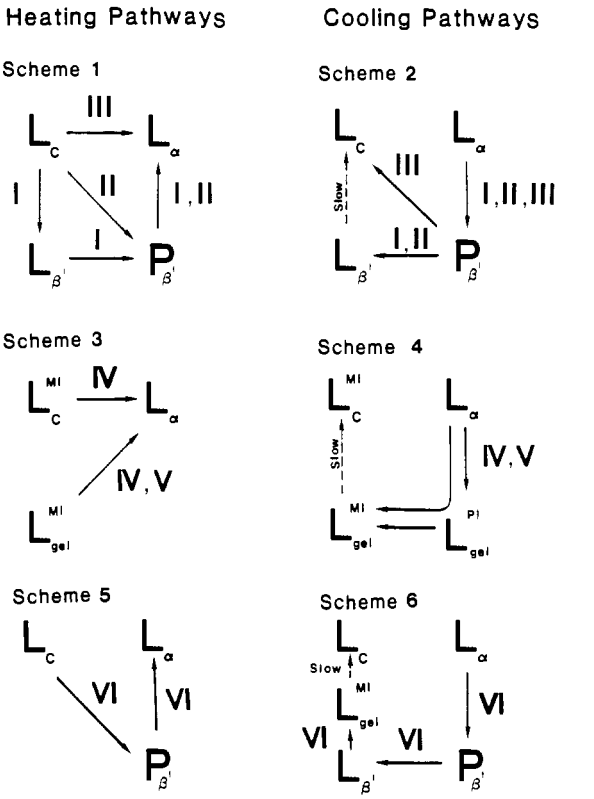

FIGURE 10: Proposed heating and cooling pathways for aqueous dispersions of various phospholipids under study. In schemes 1 and 2, lipid class I refers to C(17):C(17)PC and C(18):C(16)PC; class II refers to C(16):C(18)PC, C(15):C(19)PC, C(14):C(20)PC, and C(19):C(15)PC; class III refers to C(13):C(21)PC. In schemes 3 and 4, lipid class IV refers to C(12):C(22)PC and C(21):C(13)PC, and class V refers to C(22):C(12)PC. In schemes 5 and 6, lipid class VI refers to C(20):C(14)PC. L_c, $L_{\beta'}$, $P_{\beta'}$, and L_α denote the subgel crystalline, tilted gel, periodic ripple, and liquid-crystalline phases, respectively.

These values of ΔH together with the values of ΔS are presented in Table I. When these thermodynamic parameters are plotted against the corresponding values of $\Delta C/CL$, a linear function of ΔH or ΔS vs $\Delta C/CL$ is obtained (Figure 8B). Beyond $\Delta C/CL = 0.40$, the cooling thermograms for C(12):C(22)PC, C(21):C(13)PC, and C(22):C(12)PC are characterized by two overlapped peaks; hence, the values of ΔH and ΔS associated with the liquid-crystalline to the interdigitated gel phase cannot be determined unambiguously.

However, the values of ΔH calculated from the heating curves are 11.4, 12.0, and 13.5 kcal/mol, respectively. Clearly, they deviate from the linear plot shown in Figure 8B.

The proposed heating and cooling pathways for the various phosphatidylcholines under study are embodied in Figure 10. For phopsphatidylcholines with $\Delta C/CL < 0.4$, the suggested heating and cooling pathways are illustrated in schemes 1 and 2, respectively. Here, it is shown that the heating and cooling transitions proceed via simpler pathways as one of the two acyl chains in the mixed-chain lipid is progressively shortened. For instance, the $L_{\beta'}$ phase is absent in the heating pathway for lipid species in which one acyl chain has 13 or 14 C–C bond lengths. C(16):C(18)PC is included in this class of phospholipids, since the *sn*-1 chain, as discussed earlier, is considered to be shortened by one C–C bond length. As one of the two acyl chains is further shortened to have 12 C–C bond lengths such as C(13):C(21)PC, both the $L_{\beta'}$ and $P_{\beta'}$ phases are apparently eliminated from the heating pathway; in addition, the $L_{\beta'}$ phase is also absent in the proposed cooling pathway. Long identical-chain phosphatidylcholines such as C(16):C(16)PC and C(17):C(17)PC with the headgroup area slightly larger than the averaged cross-sectional area of the two acyl chains tend to adopt a tilted chain orientation in lamellae as demonstrated by the $L_{\beta'}$ and $P_{\beta'}$ phases (McIntosh, 1980). The absence of $L_{\beta'}$ and $P_{\beta'}$ phases in bilayers of short mixed-chain phosphatidylcholines at $T < T_m$ implies that the effective total cross-sectional area of the two acyl chains has increased so that it can match well with the polar headgroup area. This increase in the effective total cross-sectional area of the two acyl chains for short mixed-chain phosphatidylcholines is most likely caused by a more disordered dynamic structure of the lipid molecule in the gel-state bilayer. Consequently, the gradual disappearance of $L_{\beta'}$ and $P_{\beta'}$ phases shown in schemes 1 and 2 in Figure 10 is complementary to the observed linear decrease in ΔS with increasing $\Delta C/CL$ for the same series of mixed-chain lipids during the transition as shown earlier in Figure 8B.

Schemes 3 and 4 in Figure 10 show the proposed heating and cooling pathways for phospholipids with $\Delta C/CL$ = 0.44–0.55. The heating pathway has been discussed previously for mixed-chain phospholipids with similar values of $\Delta C/CL$ (Boggs & Mason, 1986; Mattai et al., 1987). Here, we introduce an intermediate phase, L_{gel}^{PI}, in the suggested cooling pathway. High-pressured infrared spectroscopic study of C(18):C(10)PC ($\Delta C/CL$ = 0.57) has shown that the lamellar C(18):C(10)PCs in the L_α phase can undergo two isothermal phase transitions upon elevation of pressure at room temperature (Wong & Huang, 1989). The first pressure-induced isothermal transition occurs at the critical pressure of 1.4 kbar, corresponding to the $L_\alpha \rightarrow L_{gel}^{PI}$ phase transition, where L_{gel}^{PI} is the gel-state bilayer in which the asymmetric chains of C(18):C(10)PC are partially interdigitated. The second pressure-induced transitions occur at 5.5 kbar, corresponding to the $L_{gel}^{PI} \rightarrow L_{gel}^{MI}$ transition, where L_{gel}^{MI} is the mixed-interdigitated gel bilayer. Since an increase in pressure acts in a manner similar to a decrease in temperature by exerting an ordering effect on the acyl chain packing in the bilayer, we therefore propose that the L_{gel}^{PI} phase observed in the high-pressure study is presumably an intermediate phase in the DSC cooling pathway and that the L_{gel}^{MI} phase promotes or catalyzes the direct conversion of the L_α phase of the L_{gel}^{MI} phase.

Figure 10 also shows the proposed heating and cooling pathways for C(20):C(14)PC. The heating pathway, scheme 5, is identical with that proposed for other mixed-chain phosphatidylcholines with a C(14) acyl chain (scheme 1). The cooling pathway, however, includes an additional state, the metastable L_{gel}^{MI} phase (scheme 6). Since the normalized chain-length difference between the two acyl chains in C(20):C(14)PC is 0.4, it is quite possible that C(20):C(14)PC molecules in the $L_{\beta'}$ phase tend to transform into a mixed-interdigitated bilayer (L_{gel}^{MI}) at low temperatures. However, the sum of the two shorter C(14) chains is longer than the full length of the longer C(20) chain in an all-trans conformation by about four C–C bond lengths. Consequently, the effective thickness of two opposing C(14) chains cannot match very well with the neighboring C(20) chain in the L_{gel}^{MI} state. The proposed mixed-interdigitated bilayer of C(20):C(14)PC, therefore, cannot be stable, and it will convert spontaneously at low temperatures to the more stable L_c phase in which the longer C(20) chain molecule from one leaflet pairs with the shorter C(14) chain of another lipid molecule contributed by the opposing leaflet.

In summary, we have demonstrated in this study that the transition entropy and other thermodynamic parameters associated with the main phase transition for aqueous dispersions of a large number of identical molecular weight phosphatidylcholines are inversely related to $\Delta C/CL$ when the values of $\Delta C/CL$ are in the range of 0.1–0.4. This linear function with negative slope suggests that the lipid–lipid interactions of phosphatidylcholines in the gel-state bilayer are perturbed progressively by an increased chain-length inequivalence. When the value of $\Delta C/CL$ reaches the range of 0.44–0.57, the perturbation is so overwhelming that the lipid molecules in the bilayer have to assume a new equilibrium position, resulting in a mixed-interdigited packing mode. Finally, it should perhaps be noted here that the proposed transition pathways for various mixed-chain phosphatidylcholines shown in Figure 10 are consistent with the observed thermotropic phase behavior for various aqueous dispersions prepared from these mixed-chain lipids. The identification of the suggested various phases, however, requires future detailed studies using other physical techniques.

References

Ali, S., Lin, H., Bittman, R. & Huang, C. (1989) *Biochemistry 28*, 522–528.

Boggs, J. M., & Mason, J. T. (1986) *Biochim. Biophys. Acta 863*, 231–242.

Chen, S. C., Sturtevant, J. M., & Gaffney, B. J. (1980) *Proc. Natl. Acad. Sci. U.S.A. 77*, 5060–5063.

Finegold, L., & Singer, M. A. (1984) *Chem. Phys. Lipids 35*, 291–297.

Gomori, G. (1942) *J. Lab. Clin. Med. 27*, 952–959.

Huang, C. (1990) *Klin. Wochenschr. 68*, 149–165.

Huang, C., & Levin, I. W. (1983) *J. Phys. Chem. 87*, 1509–1513.

Huang, C., & Mason, J. T. (1986) *Biochim. Biophys. Acta 864*, 423–470.

Hui, S. W., Mason, J. T., & Huang, C. (1984) *Biochemistry 23*, 5570–5577.

Lewis, R. N. A. H., Mak, N., & McElhaney, R. N. (1987) *Biochemistry 26*, 6118–6126.

Lin, H., & Huang, C. (1988) *Biochim. Biophys. Acta 946*, 178–184.

Mason, J. T., & Huang, C. (1981) *Lipids 16*, 604–608.

Mason, J. T., Broccoli, A. V., & Huang, C. (1981) *Anal. Biochem. 11*, 96–101.

Mattai, J., Scripada, P. K., & Shipley, G. (1987) *Biochemistry 26*, 3287–3297.

McIntosh, T. J. (1980) *Biophys. J. 29*, 237–246.

McIntosh, T. J., Simon, S. A., Ellington, J. C., Jr., & Porter,

N. A. (1984) *Biochemistry 23*, 4038-4044.
Mena, P. L., & Djerassi, C. (1985) *Chem. Phys. Lipids 37*, 257-270.
Shah, J., Scripada, P. K., & Shipley, G. G. (1990) *Biochemistry 29*, 4254-4262.
Slater, J. L., & Huang, C. (1988) *Prog. Lipid Res. 27*, 325-359.
Stümpel, J., Eibl, H., & Nicksch, A. (1983) *Biochim. Biophys. Acta 727*, 246-254.
Wong, P. T. T., & Huang, C. (1989) *Biochemistry 28*, 1259-1263.
Wu, W., Chong, P. L., & Huang, C. (1985) *Biophys. J. 47*, 237-242.
Xu, H., & Huang, C. (1987) *Biochemistry 26*, 1036-1043.
Zaccai, G., Büldt, G., Seelig, A., & Seelig, J. (1979) *J. Mol. Biol. 134*, 693-706.

Differential Scanning Calorimetric Study of a Homologous Series of Fully Hydrated Saturated Mixed-Chain C(X):C(X+6) Phosphatidylcholines†

Zhao-qing Wang, Hai-nan Lin, and Ching-hsien Huang*
Department of Biochemistry, Health Sciences Center, University of Virginia, Charlottesville, Virginia 22908
Received February 20, 1990; Revised Manuscript Received April 20, 1990

ABSTRACT: The successive high-resolution differential scanning calorimetric (DSC) thermograms for aqueous dispersions of a homologous series of mixed-chain phosphatidylcholines, C(X):C(X+6)PC, have been recorded and analyzed. In this series of saturated mixed-chain phosphatidylcholines, the total number of carbon atoms in the *sn*-1 acyl chain increases from 11 to 20, and the *sn*-2 acyl chain is always 6 methylene units longer than the *sn*-1 acyl chain. In the initial heating DSC thermograms, two prominent endothermic transitions are detected for all the samples prepared from the various C(X):C(X+6)PCs except C(12):C(18)PC. In contrast, a single exothermic transition is observed on cooling for all the samples except C(13):C(19)PC. The temperature difference between the two endothermic transitions increases linearly as the acyl chain length of C(X):C(X+6)PC becomes progressively longer. Interestingly, the main phase transition occurs before the subtransition for C(11):C(17)PC dispersions. Our DSC data further demonstrate that the thermodynamic parameters (T_m, ΔH, and ΔS) associated with the main phase transition for fully hydrated C(13):C(19)PC and other identical MW phosphatidylcholines are inversely related to the corresponding values of the chain-length inequivalence ($\Delta C/CL$) for these lipids. This linear relationship can be employed to map the T_m values for aqueous dispersions prepared from a large number of mixed-chain phosphatidylcholines whose values of $\Delta C/CL$ are within the range of 0.1-0.4.

The systematic differential scanning calorimetric (DSC)[1] study of a homologous series of identical-chain phosphatidylcholines, C(X):C(X)PC, in excess water yields important information concerning the relative effect of chain ends on the chain packing order (Mason & Huang, 1981), the relative metastability of various lipid phases (Finegold & Singer, 1986), and the change in transition pathways as a function of chain length (Lewis et al., 1987). For instance, it has been demonstrated that fully hydrated short-chain phosphatidylcholines ($X \leq 8$) do not undergo the endothermic phase transition upon heating and that longer chain phosphatidylcholines ($X \geq 22$) do not self-assemble in excess water into the rippled gel phase ($P_{\beta'}$) at $T < T_m$. These interesting results may be of great importance in understanding the roles of various fatty acid compositions in biological membranes.

In order to extend the previous studies on identical-chain phosphatidylcholines, we have carried out the DSC study of a homologous series of mixed-chain phosphatidylcholines, C(X):C(X+6)PC, in which the *sn*-2 acyl chain is chosen to be 6 methylene units longer than the *sn*-1 acyl chain, and the total number of carbon atoms in the *sn*-1 acyl chain, X, increases systematically from 11 to 20. Although the *sn*-2 acyl chain in the fully extended conformation is always six methylene units longer than the *sn*-1 acyl chain in this homologous series of mixed-chain phosphatidylcholines, the normalized chain-length difference or inequivalence ($\Delta C/CL$) between the *sn*-1 and *sn*-2 acyl chains for the mixed-chain phospholipid in the gel-state bilayer decreases progressively as the value of X in C(X):C(X+6)PC increases systematically. Here, ΔC is the effective chain-length difference between the *sn*-1 and *sn*-2 acyl chains in terms of C–C bonds for phospholipid molecules in the gel-state bilayer, and it is a constant value of 4.5 for C(X):C(X+6)PC. The term CL is the effective chain length of the longer of the two acyl chains in C–C bonds, and it equals $X + 3.5$ for C(X):C(X+6)PC. In calculating the value of ΔC and CL, an inherent shortening of 1.5 C–C bond lengths for the *sn*-2 acyl chain has been taken into account; this shortening is caused by a sharp bend on the *sn*-2 acyl chain at the bond between C(2) and C(3) for phospholipids in the gel-state

†This research was supported in part by U.S. Public Health Service Grant GM-17452 from the NIH, Department of Health and Human Services.

[1] Abbreviations: C(X):C(X)PC, saturated identical-chain L-α-phosphatidylcholine having X carbons in the *sn*-1 chain as well as the *sn*-2 acyl chain; C(X):C(X+6)PC, saturated mixed-chain L-α-phosphatidylcholine having X carbons in the *sn*-1 acyl chain and $X + 6$ carbons in the *sn*-2 acyl chain; DSC, differential scanning calorimetry; MW, molecular weight.

0006-2960/90/0429-7072$02.50/0